Insights into the mechanisms of nucleation and growth of C–S–H on fillers

Ouyang, Xiaowei; Koleva, D. A.; Ye, Guang; van Breugel, K.

DOI
10.1617/s11527-017-1082-y

Publication date
2017

Document Version
Final published version

Published in
Materials and Structures

Materials and Structures (2017)50:213
DOI 10.1617/s11527-017-1082-y

ORIGINAL ARTICLE

Insights into the mechanisms of nucleation and growth of C–S–H on fillers

Xiaowei Ouyang · D. A. Koleva · Guang Ye · K. van Breugel

Received: 3 February 2017 / Accepted: 19 August 2017

Abstract A complete understanding of the mechanisms upon which a filler acts in a cement-based material, e.g. as a C–S–H nucleation and/or growth-inducing factor, is of high importance. Although various studies report on accelerated cement hydration in the presence of fillers, the reason behind these observations is not completely understood yet. This work contributes to this subject, by providing an experimental evidence on the (electro) chemical aspects of the filler surface modification in the model solution, simulating the pore solution of cement paste. The nature of the various interactions with regard to the affinity of a filler surface towards C–S–H nucleation and growth was discussed in detail in this work with regard to zeta potential measurements of micronized sand and limestone particles in the model solutions. These results are further supported by microscopic observations of morphology and distribution of hydration products on the filler surfaces, together with considerations on thermodynamic principles in view of hydration products formation and distribution. The C–S–H nucleation and growth appeared to be due to the interactions between a filler surface and calcium ions in the pore solution. These interactions were determined by the chemical nature of the filler surface. The interaction mechanisms were found to be governed by relatively weak electrostatic forces in the case of micronized sand. This was reflected by a non-significant adsorption of calcium ions on the filler surface, resulting in non-uniformly distributed and less stable C–S–H nuclei. In contrast, the nucleation and growth of C–S–H on limestone particles were predominantly determined by donor–acceptor mechanisms, following moderate acid–base interactions. Consequently, a strong chemical bonding of calcium ions to a limestone surface resulted in a large amount of uniformly distributed C–S–H nuclei.

Keywords Calcium silicate hydrate (C–S–H) · Nucleation · Fillers · Zeta potential · Adsorption

1 Introduction

Portland cement is a basic component of concrete with a high environmental impact because of the high CO_2 emission and energy consumption during cement production. Fillers, such as limestone or quartz powder, are used as a replacement for Portland cement to make concrete cheaper and more environment friendly [1–3]. Additions of limestone or quartz powder have been reported to exert a limited chemical effect on cement hydration [4, 5]. The main quasi-chemical effect of added limestone and quartz powder is that they accelerate cement hydration by facilitating

X. Ouyang (✉) · D. A. Koleva · G. Ye · K. van Breugel
Materials and Environment, Faculty of Civil Engineering and Geosciences, Delft University of Technology, 2628CN Delft, The Netherlands
e-mail: x.ouyang@tudelft.nl

Published online: 23 August 2017

nucleation and growth of hydrates at their surfaces [1, 5–7]. The nucleation process depends predominantly on the active surface area of the fillers, where smaller particle size i.e. larger active surface, facilitates nucleation. The subsequent growth is determined by ionic sorption interactions, occurring at the interface between the filler particles and the hydration products, further governed by the pH and composition of the pore solution. These effects are most important in the early stage of cement hydration when the microstructure is rapidly developing. The hydrates, of which mainly calcium silicate hydrate (C–S–H), precipitate and constitute at least 60% of the fully hydrated cement paste, forming a rigid network of cement and filler grains, leading to setting and strength development.

The replacement level of a filler and its fineness are the major factors affecting the hydration kinetics [8–10]. The first effect is related to the dilution of cement, which is equivalent to an increase in the water–cement ratio. The replacement of cement by fillers means that relatively more space is available for the formation of hydrates. The hydration process is, therefore, accelerated [9, 11]. The second effect is the nucleation (heterogeneous or homogeneous) of C–S–H on the fillers' surface [10, 12]. This effect depends on: (1) the fineness of the fillers' particles, since a greater fineness means a higher specific surface area; (2) the amount of filler used, since the probability for nucleation sites increases with the amount of foreign particles; (3) the affinity of the fillers' particles for cement hydrates, which is related to the chemical nature of the filler used. Stark et al. [13] and Berodier and Scrivener [14] reported on direct observations of different nucleation and growth of C–S–H on quartz, calcite and cement surfaces. Since the chemical nature of fillers and cement is different, logically various chemical mechanisms would play a role for the divergence in the rate of C–S–H nucleation, orientation and growth on each surface. Poppe [15] and Oey et al. [10] also found that limestone affected the hydration kinetics more than quartz. Berodier and Scrivener [14] explained that the increased nucleation on limestone surfaces could be related to the dissolution of the limestone phase, but also to a favorable surface structure, providing a "template" for C–S–H precipitation. Oey et al. [10] had put forward the hypothesis that calcite (i.e. limestone) provides a lower energy barrier for C–S–H nucleation than quartz. Furthermore, dissolved CO_3^{2-} ions, released from calcite, would adsorb on C–S–H, followed by OH^- ions release into the pore solution. The consequence would be a concentration gradient, which enhances the rate of C–S–H growth and potentially accelerates cement hydration. Despite the reported experimental evidence, there are no reports on the reasons behind the observed behaviour in view of (electro)chemical transformations (and charge respectively) on the surface of fillers and/or changes in the chemical kinetics of cement hydration in their presence. Additionally, to what extent the surface area, ion exchange and interfacial interactions overall would depend on, or be determined by, the electrical charge of the filler particle is so far not addressed in the state of the art.

This paper contributes to answering the above posed questions and communicated hypothetical mechanisms by studying the charge of fillers' particles in model medium. The paper reports on investigating the effects of surface properties, and related ionic charge interactions of fillers' particles, on the nucleation and growth of C–S–H on their surface. Two types of fillers were tested: micronized sand and limestone powder. Microscopic observations of the nucleation and growth of C–S–H on the surface of these filler particles were performed by scanning electron microscopy (SEM). In parallel to the microscopic observations, the surface charge properties of cement and fillers were studied via zeta potential measurements in model solutions. The relation between the chemical nature of the fillers and the nucleation and growth of C–S–H is discussed, emphasizing on the mechanisms, responsible for the actual C–S–H nucleation and growth in the presence of fillers and cement particles.

2 Materials and methods

2.1 Materials and mixture

The cement used in this study was ordinary Portland cement (OPC) CEM I 42.5 N, produced by ENCI, The Netherlands. The fillers used were limestone powder (LP) and micronized sand (MS). The LP had an average particle size of 9 μm, while the MS had a particle size of 13 μm. The chemical composition of the fillers and Portland cement is listed in Table 1. The mineral composition of OPC was calculated by the

Table 1 Chemical composition (% by mass) of cement and fillers

Name	OPC	Limestone powder	Micronized sand
CaO	64.40	–	0.02
SiO_2	20.36	0.34	99.5
Al_2O_3	4.96	0.2	0.20
Fe_2O_3	3.17	0.07	0.03
K_2O	0.64	0.01	0.04
Na_2O	0.14	0.02	–
SO_3	2.57	0.05	–
MgO	2.09	0.27	–
$CaCO_3$	–	97.46	–

Table 2 Mineral composition of cement (% by weight)

Phase	C_3S	C_2S	C_3A	C_4AF
Weight (%)	67.1	5.9	7.8	9.6

Bogue equation [16] and is shown in Table 2. To maintain the nucleation and growth of C–S–H on the surface of both fillers in constant and identical conditions, only one mixture was prepared by mixing OPC, LP, MS and water, denoted as OPC–LP–MS. The percentage of different fillers and the water to binder ratio are given in Table 3. The mixture was prepared in a Hobart mixer according to the standard procedures described in ASTM C305 [17]. After mixing, the fresh paste was cast into bottles (33 mm diameter, 70 mm height), sealed and stored in the laboratory at 20 ± 2 °C until used.

2.2 Cement paste filtrate analysis

A VARIAN Vista 720 ICP-OES was used to analyse the elemental concentrations in cement paste filtrates. The filtrate of the fresh cement paste was collected at each required time by vacuum filtration using 0.22 μm filter paper. The cement paste filtrates were then stored in sealed 20 mL plastic vials until used.

2.3 SEM analysis

ESEM Philips XL 30 was used for morphological investigation of the hydration products on the surface of fillers and cement particles. The sample preparation for SEM analysis was performed according generally reported procedures [14], as follows: at each required time interval, about 1 g of the OPC–LP–MS paste was taken from the sealed bottle to stop hydration by solvent exchange with isopropanol; after stopping cement hydration and removing the isopropanol, the paste collapsed to a dried powder; the dried powder was then collected and stored under vacuum in a desiccator until used. SEM observations were performed on the dried powder coated by carbon. SE mode was used.

2.4 Zeta potential test

2.4.1 Preparation of suspensions

The zeta potential tests for the various particles in this study were performed in five series of model solutions. The detailed chemical composition of the five model solutions is shown in Table 4. The zeta potential of MS and LP particles was initially measured in aqueous NaOH solutions with different concentrations, where the pH of the NaOH solutions were 8, 9, 10, 11, and 12, respectively. On the other side, in order to evaluate the effect of different concentrations of Ca^{2+}, Na^+, K^+, SO_4^{2-} ions on the charge of the tested filler particles, the zeta potential measurements were also performed separately for the MS and LP particles suspended in solutions with different concentrations of $Ca(OH)_2$, and in mixture solutions of $Ca(OH)_2$ + NaOH, $Ca(OH)_2$ + KOH, and $Ca(OH)_2$ + K_2SO_4.

For the aqueous $Ca(OH)_2$ solutions series, the tested Ca^{2+} concentrations were from 0.2 to 20 mmol/L, which were obtained by diluting a saturated lime solution ($[Ca^{2+}]$ = 22 mmol/L). In this case, the pH of the Ca-solutions were varied from 9.2 to 12.3 at 25 °C (Table 4). For mixtures solutions, different

Table 3 Mixture compositions of blended cement paste

Mixture	OPC[a](%)	Limestone powder [a](%)	Micronized sand [a](%)	w/b[b]
OPC–LP–MS	60	20	20	0.4

[a] Percentage of the total mass of binder by weight

[b] w/b represents water to binder ratio

Table 4 Preparation of model solutions (the concentrations are shown in mmol/L units)

Solution 1		Solution 2		Solution 3		Solution 4		Solution 5	
NaOH	pH	$Ca(OH)_2$	pH	$Ca(OH)_2$	NaOH	$Ca(OH)_2$	KOH	$Ca(OH)_2$	K_2SO_4
–	8	0.2	9.2	0.1	10	0.1	10	0.1	10
–	9	0.4	9.3	0.4	10	0.4	10	0.4	10
–	10	0.6	9.6	1	10	1	10	1	10
–	11	0.8	10.1	4	10	4	10	4	10
–	12	1	10.5	8	10	8	10	8	10
–	–	2	10.8	0.1	50	0.1	50	10	10
–	–	4	10.9	0.4	50	0.4	50	15	10
–	–	6	11.0	1	50	1	50	19.6	10
–	–	8	11.9	4	50	4	50	0.1	50
–	–	10	12.0	8	50	8	50	0.4	50
–	–	15	12.2	–	–	–	–	1	50
–	–	20	12.3	–	–	–	–	4	50
–	–	–	–	–	–	–	–	8	50
–	–	–	–	–	–	–	–	10	50
–	–	–	–	–	–	–	–	15	50
–	–	–	–	–	–	–	–	18	50

concentrations of aqueous of $Ca(OH)_2$ solutions (from 0.1 to 19.6 mmol/L) were firstly prepared and then defined solid salts weights of a OH, KOH or K_2SO_4 were dissolved in the mixture solutions. For each Ca-concentration in the mixture solutions, the considered concentrations of NaOH, KOH or K_2SO_4 were 10 and 50 mmol/L, as shown in Table 4.

2.4.2 *Zeta potential measurements*

The zeta potential of particles in solution is measured by applying a controlled electric field, as schematically illustrated in Fig. 1, by means of electrodes immersed in the sample suspension. This causes the charged particles to move towards the electrode of opposite charge. Viscous forces, acting on the particle in motion, tend to oppose this movement, establishing a balance between the forces of electrostatic attraction and viscous drag. The zeta potential can be calculated based on this electrophoretic mobility.

In this study, the zeta potential of MS and LP filler particles in model solutions was measured by Malvern Zetasizer Nano (Z-ZS-ZSP) (Malvern instruments Ltd., UK). Five runs were conducted for each sample, with the average value being taken as the final result. This technique is appropriate, but also has limitations, e.g. at low or high pH values of the medium, which restricts the range of species concentration in the electrolyte. If these concentrations are too high, the electrical conductivity of the electrolyte increases and erroneous results can be obtained. In this work, the upper electrolyte concentration limit corresponds roughly to 50 mmol/L in K_2SO_4.

2.5 Technical background on zeta potential and considerations related to (electro)chemical surface modifications on filler phases

The zeta potential (ζ) is a measure of charge, carried by particles suspended in a liquid. As shown in Fig. 1,

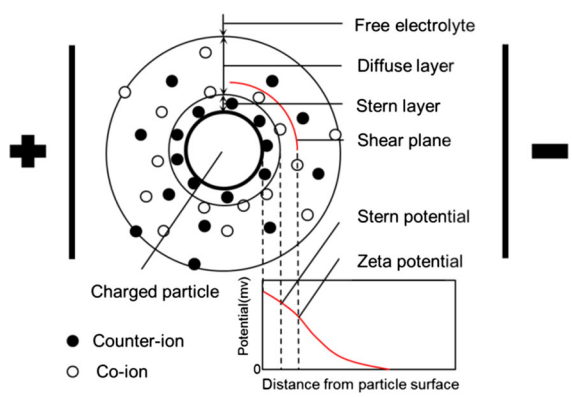

Fig. 1 Schematic illustration of the electrical double layer and zeta potential test

a charged particle surface attracts a layer (Stern layer [18]) of counter-ions (ions of opposite charge) from the aqueous phase. Due to ionic ratio constraints, the strongly adsorbed counter-ions will not fully offset the surface charge. A second layer (diffuse layer) of more loosely attracted counter-ions forms subsequently. At a certain distance from the particle surface, the surface charge will be fully balanced by counter-ions. Within the diffuse layer, there is a notional boundary (the shear plane in Fig. 1) inside which the ions and particles form a stable entity. In fact, when a particle moves, ions at this boundary cause this movement. The ions beyond the boundary remain in the bulk dispersant. The potential at the location of this shear plane is the zeta potential, which is the reflection of the surface charge of the particle.

Two concepts are very important related to zeta potential. One is the point of zero charge (PZC). It corresponds to the conditions in which the surface charge of the solid is equal to zero and does not necessarily correspond to a zeta potential $\zeta = 0$. The other one is the iso-electric point (IEP). It corresponds to a zeta potential $\zeta = 0$ and hence to a zero electrophoretic mobility, but not necessarily to a zero surface charge. Generally, when ions, different from those in the lattice ions of the system, are present in the solution (e.g. for $CaCO_3$ ions such are SO_4^{2-}, Mg^{2+}), the IEP is different from the PZC. In the absence of ion adsorption from the solution (ions, different from the crystal's lattice ions), the IEP and the PZC are similar [19, 20].

The surface charge of suspended particles is influenced by the adsorption reactions on these surfaces. Furthermore, the rates of processes such as dissolution of mineral phases (of importance in the weathering of rocks), precipitation (heterogeneous nucleation and crystal growth) and ion exchange depend on the reactivity of surfaces and their molecular (atomic) surface structures which in turn are influenced by adsorption of ions on these surfaces [21]. There are two main paths in the adsorption reactions. One is the chemical interaction of solutes with the tested surfaces, by formation of coordinative bonds. The other one is due to electrical interactions of the solutes with the solid surfaces, such as electrostatics interactions and polarization interactions [22]. With regard to this work, the following needs to be considered: C–S–H is formed by similar dissolution–precipitation process during the hydration of cement. The presence of fillers affects these processes, in view of the heterogeneous nucleation and crystal growth of C–S–H, by different adsorption reactions on these fillers and depending on the surface chemical characteristics. The adsorption reactions in turn affect the surface charge of these fillers. In other words, the surface adsorption reactions are linked to alterations of surface charge and consequently related to hydration products nucleation and growth. The surface charge is reflected by the zeta potential of the particles of interest in relevant conditions. Therefore, the variation of zeta potential in conditions of interest can further elucidate the conditions upon which variation of C–S–H nucleation and growth occurs on different filler particles.

3 Results and discussion

3.1 Chemical composition of cement paste filtrate

Table 5 lists the chemical composition of the filtrate of the blended cement paste. It is inferred that upon contact with water ions go into solution quickly. Within 10 min, the concentration of Na^+, K^+, SO_4^{2-}, Ca^{2+} increases significantly. The silicate concentration is very low and the aluminate concentration is even lower, despite the high reactivity of the aluminate phase of the clinker. This is in accordance to generally reported pore solution composition, where predominantly K^+ and Na^+ are present, with lower amounts of Ca^{2+} [23]. Since the liquid phase of cement paste at early stage mainly consists of Na^+, K^+, SO_4^{2-} and

Table 5 Elemental concentrations for cement paste filtrate

Time	Na (mM)	K (mM)	S (mM)	Si (μM)	Al (μM)	Ca (mM)
10 min	79.0	180.8	81.3	46.4	<37.0	11.8
30 min	79.1	175.5	70.9	39.3	<37.0	15.7
1 h	80.1	180.6	65.7	39.3	<37.0	16.6
3 h	94.2	200.7	77.5	142.9	<37.0	16.1

Ca^{2+}, we used lime, alkali hydroxides, or alkali sulfate solutions as the liquid phase to investigate the zeta potential of MS and LP fillers.

3.2 Zeta potential

3.2.1 Effect of pH

The evolution of the zeta potential of MS and LP particles as a function of pH was determined in a series of model solutions (Table 4). The results for NaOH solution (solution 1, as shown in Table 4) are presented in Fig. 2. In acidic medium, LP particles could dissolve and generate CO_2 which would cause an adverse impact on the results. Therefore, the measurements in NaOH solution in the pH range from 8 to 12 were performed, in order to obtain an overall information on the zeta potential values of MS and LP from close to neutral (pH 7) to an alkaline medium.

As can be seen in Fig. 2, the zeta potential of both MS and LP particles in the range of pH 8–12 was negative i.e. between −20 and −56 mV. While the zeta potential values for LP remained stable and around −20 mV between pH 8 and pH 11, the zeta potential for the MS particles presented an increase in negative charge, reaching ca. −60 mV at pH 11. The potential for LP particles remained more positive than that for the MS particles in the full pH range of this test. The values recorded at pH 12 are slightly different from these at pH 11: more positive for LP and similar to pH 11 for MS. Since these values would be affected by interference within the measurement itself (mainly due to a normally observed abrupt increase of the ionic strength/conductivity of the solution in ranges of pH below 2 and higher than 11.5), the results at pH 12 are considered as indicative, rather than as absolute values.

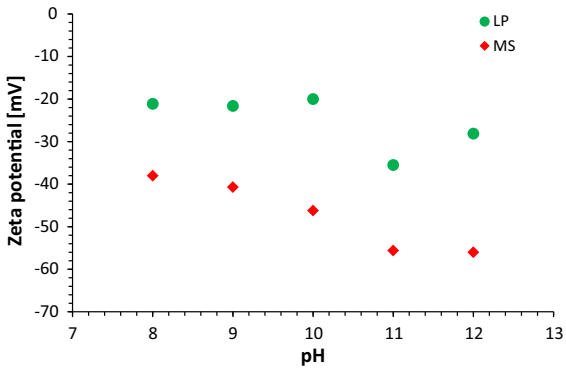

Fig. 2 Evolution of the zeta potential of MS and LP particles as a function of pH in NaOH solution

With regard to MS particles, the main cause of surface charge generation at the silicate–solution interface is due to dissociation of the silanol groups at this interface. The dissociation is related to gain or loss of a proton, which depends on the pH value of the aqueous phase [24, 25]. The silanol groups in pure water dissociate through the following reactions [21, 26]:

$$\equiv SiOH + H^+ \rightleftharpoons \equiv SiOH_2^+ \quad (1)$$

$$\equiv SiOH + OH^- \rightleftharpoons \equiv SiO^- + H_2O \quad (2)$$

The H^+ and OH^- ions are the potential determining ions for silica. With an increase of pH, more silanol groups are ionized and the surface charge of silica and hence becomes more negative.

Different from the generation of surface charge on silica, which corresponds to ionization of surface silanol groups, the surface charge of calcite is associated with surface defects. There are three groups of main surface defects [19]: (1) Structural defects of the crystal lattice; (2) Defects due to ions exchange involving ions in the crystal lattice and the ions in solution; (3) Defects, following chemical reactions on the surface with constitutive ions or adsorption on the external face. The principal mechanism of charge development at the calcite–water interface is assumed to be a preferential hydrolysis of surface calcium and carbonate ions, followed by the adsorption of the resulting complexes at the surface [27]. Additionally, previous studies [19, 28, 29] showed that the zeta-potential determining ions for calcite are Ca^{2+} and CO_3^{2-}, i.e. the crystal-constituting species, whereas pH seems to be a second-order controlling parameter through its influence on the CO_3^{2-}/HCO_3^- and $Ca^{2+}/CaOH^+$ speciation, both in the solution, as well as at the calcite/water interface. Therefore, unlike silica, H^+ and OH^- are generally not considered as zeta potential determining ions for calcite [30].

As can be seen in Fig. 2, the zeta potential of calcite (LP particles) did not significantly vary between $8 > pH = 11$, while present a gradually increasing negative charge for the MS particles (as above discussed) in identical solutions. Other authors have reported the same conclusion for LP [31]. The variation of zeta potential as a function of pH for the

LP particles likely caused by the equilibrium of the dissolution of calcium and carbonate ions, and the adsorption of the complexes formed at the calcite/water interface.

3.2.2 *Effect of Ca^{2+} concentration*

The zeta potential of LP and MS particles in solutions of $Ca(OH)_2$ (solution 2, as shown in Table 4) was measured as a function of Ca^{2+} concentration and compared to the zeta potential of OPC particles measured by Nachbaur et al. [32] and C–S–H particles measured by Viallis-Terrisse et al. [33] and Nachbaur et al. [32], respectively. The results of measured zeta potential are depicted in Fig. 3. As can be observed, for OPC, MS and C–S–H particles a similar isoelectric point (IEP) was recorded, which was reached at a Ca^{2+} concentration of about 2 mmol/L. This is because of the fact that the OPC, MS and C–S–H particles are very rich in silicate phase, as aforementioned and also reported in [32]. At very low Ca^{2+} concentrations, the silica layers are partially ionized as SiO^- groups, leading to an overall negative zeta potential if no counter ions are specifically adsorbed. As previously outlined, adsorption plays an important role within the surface charge interaction on a particle surface. At higher Ca^{2+} concentrations, but still lower than 2 mmol/L, adsorption of Ca^{2+} ions onto the surfaces of OPC, MS and C–S–H particles partially compensates for this negative charge, resulting in lower absolute values of zeta potential. When the Ca^{2+} concentrations are higher than 2 mmol/L, the adsorption of Ca^{2+} overcompensates for the surface charge, leading to reversal of the zeta potential. The zeta potential of the MS particles, hence, was positive in conditions of Ca^{2+} concentration higher than 2 mmol/L.

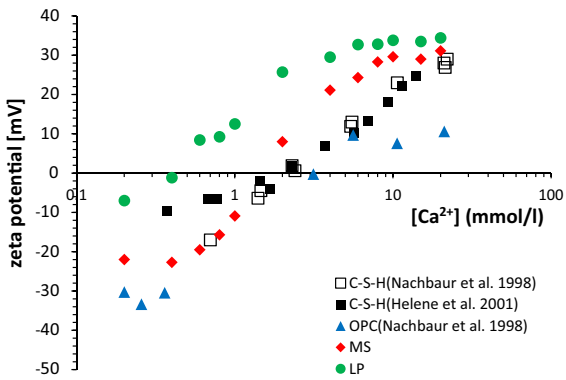

Fig. 3 Evolution of the zeta potential of OPC, MS, C–S–H and LP particles as a function of Ca^{2+} concentration in $Ca(OH)_2$ Solution

The evolution of zeta potential versus Ca^{2+} concentration for the LP particles shows a different trend compared to OPC, MS and C–S–H particles. A much lower Ca^{2+} concentration was needed for the LP particles to reach the IEP, which was about 0.4 mmol/L. Compared to the zeta potential of LP particles in NaOH solution at pH of 9, 10, 11 and 12 (Fig. 2), the zeta potential in $Ca(OH)_2$ was more positive for the same pH. According to the reported mechanisms of charge development at the calcite/solution interface [19, 27–29], it could be stated that in NaOH solution of pH > 8, the zeta potential of the LP particles was dominated by hydrolysis of calcium ions on the particles' surface, leading to an overall negative zeta potential (Fig. 2). In other words, at pH of about 9 and at very low Ca^{2+} concentrations in the solution phase (<0.4 mmol/L for the $Ca(OH)_2$ solution and 0 mmol/L for the NaOH solution), the hydrolysis of surface calcium ions dominated the acquired zeta potential. Upon increase of the Ca^{2+} concentration, the zeta-potential shifted to more positive values as a result of Ca^{2+} adsorption on the particles surface (Fig. 3). At higher Ca^{2+} concentrations (>0.4 mmol/L), adsorption of external, rather than hydrolysis of surface Ca^{2+} ions dominated the surface charge, leading to a "reversal" of the zeta potential. As the Ca^{2+} concentration increased from 0.4 to about 6 mmol/L, the amount of the Ca^{2+} ions adsorbed onto the LP surface would gradually increase, which was reflected by an increase in the zeta potential (Fig. 3). The plateau region at concentrations higher than 6.00 mmol/L, Fig. 3, indicates stabilisation of the zeta-potential and independence of further increase of the calcium ions concentration. This reflects a stage at which a saturation condition was reached for the LP surface.

At a given Ca^{2+} concentration, the recorded zeta potential for LP particles appeared to be more positive, if compared to the recorded values for OPC, MS and C–S–H particles. These results indicate that the surface of LP particles has more affinity for Ca^{2+} compared to the surface of OPC, MS and C–S–H particles. This point will be discussed in more details in Sect. 3.2.4.

3.2.3 *Effect of Na^+ and K^+ concentration*

The evolution of the zeta potential of MS, C–S–H and LP particles in NaOH and KOH solutions (solution 3 and 4, as shown in Table 4) as a function of calcium content is presented in Figs. 4 and 5, respectively. It was observed that at low concentrations (10 mmol/L) of NaOH and KOH solutions, the development of the zeta potential of MS, C–S–H and LP particles as a function of Ca^{2+} concentration (Figs. 4, 5) remained similar to that, measured in the Na^+ and K^+-free, $Ca(OH)_2$ solutions (Fig. 3). For the MS and C–S–H particles a similar IEP was recorded, regardless the used solutions (Figs. 4, 5). This is due to the rich silicate phase on the surfaces of both MS and C–S–H particles, as mentioned previously. The IEP for MS and C–S–H particles in NaOH and KOH, similarly to $Ca(OH)_2$ solutions, was observed in the range of ca. 2 mmol/L Ca^{2+} concentration, while for the LP particles it was again expressed at Ca^{2+} concentration of ca. 0.4 mmol/L. However, at a high concentration (50 mmol/L) of NaOH and KOH solutions, the IEP for MS, C–S–H and LP particles seems to be shifted slightly towards higher Ca^{2+} concentrations. Therefore, sodium and potassium are believed to be "indifferent" ions. Nachbaur et al. [32] made the same point. The zeta potential of LP and MS particles varies almost linearly with the log of Ca^{2+} concentration near the IEP, and the latter is shifted to higher Ca^{2+} concentration. This indicates that as the Ca^{2+} concentration increased, the amount of Ca^{2+} ions, adsorbed on the MS and LP surface increased gradually, accompanied by an increase in the zeta potential. Furthermore, these changes suggest that the surface of LP particles have a larger affinity for Ca^{2+} compared to the surface of MS particles, as previously hypothesized in Sect. 3.2.2. This point will be discussed in more details in Sect. 3.2.4.

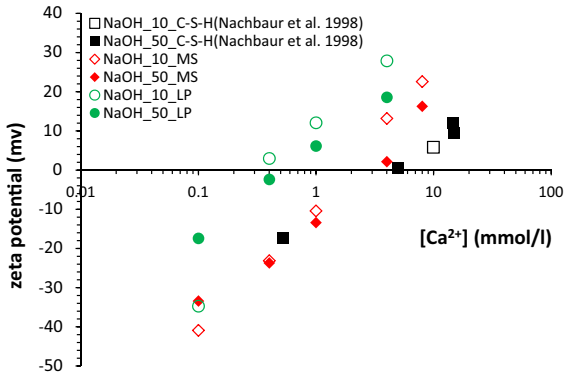

Fig. 4 Evolution of the zeta potential of MS, C–S–H and LP particles as a function of Ca^{2+} concentration in 10 and 50 mmol/L NaOH solutions

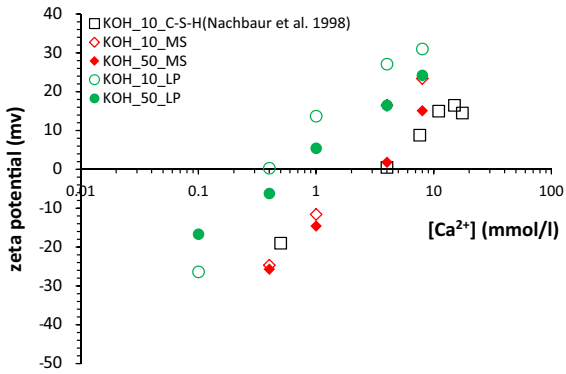

Fig. 5 Evolution of the zeta potential of MS, C–S–H and LP particles as a function of Ca^{2+} concentration in 10 and 50 mmol/L KOH solutions

3.2.4 *Effect of SO_4^{2-} concentration*

The evolution of the zeta potential of MS, C–S–H and LP particles as a function of Ca^{2+} concentration in potassium sulfate solutions (solution 5, as shown in Table 4) is illustrated in Fig. 6. It was found that, there was almost no difference between the behavior of MS and C–S–H particles, due to the rich silicate phase on the surfaces of both MS and C–S–H particles. The zeta potential of MS and C–S–H particles varied linearly with the log of Ca^{2+} concentration, and shifted to

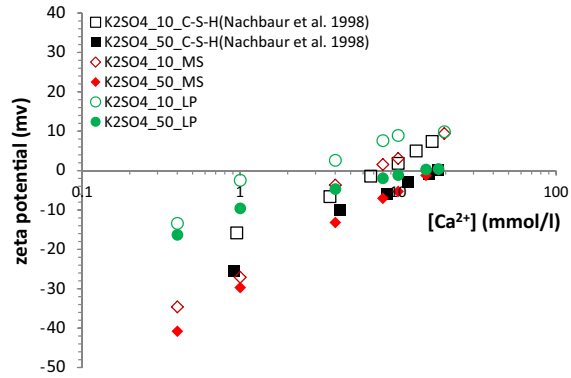

Fig. 6 Evolution of the zeta potential of MS, C–S–H and LP particles as a function of Ca^{2+} concentration in 10 and 50 mmol/L K_2SO_4 solutions

higher Ca^{2+} concentration as the sulfate concentration increased. With an increase of the sulfate concentration the IEP for MS and C–S–H particle also changed to values corresponding to higher Ca^{2+} concentration. It is interesting to note that when the sulfate concentration is 10 mmol/L, the IEP for MS and C–S–H is also about 10 mmol/L. This means that SO_4^{2-} and Ca^{2+} are equally adsorbed on MS and C–S–H surfaces. The observed linear relation of zeta potential/log Ca^{2+} concentration and the simultaneously occurring shift to higher Ca^{2+} concentration as the sulfate concentration increased, confirms that the adsorption reactions of SO_4^{2-} and Ca^{2+} onto MS and C–S–H surfaces are similar.

By contrast, in the case of LP particles, the zeta potential varied non-linearly with the log of Ca^{2+} concentration. As shown in Fig. 6, the change in zeta-potential values for LP becomes not significant with an increase of Ca^{2+} concentration and stabilises around zero in the 50 mmol/L K_2SO_4 solution with high Ca^{2+} concentration (>10 mmol/L). This is due to the Langmuir type of adsorption of ions on the calcite surface, as previously discussed and reported in [28]. Furthermore, different from the MS and C–S–H particles, for which the IEP was reached at equal SO_4^{2-} and Ca^{2+} concentration, the IEP of the LP particles was observed when the SO_4^{2-} concentration was much higher than that of Ca^{2+}. As shown in Fig. 6, the IEP for LP appeared at Ca^{2+} concentration of about 2 mmol/L in 10 mmol/L K_2SO_4 solution, and at about 0 mmol/L for the 50 mmol/L K_2SO_4 solution. This is attributed to the fact that calcite surfaces have higher affinity for Ca^{2+} ions than SO_4^{2-} ions, as previously reported by Pourchet et al. [34], who conducted a study on SO_4^{2-} and Ca^{2+} ions adsorption on calcite. The results showed that when both SO_4^{2-} and Ca^{2+} ions adsorption on calcite reached a saturation point, the amount of adsorbed SO_4^{2-} ions represents approximately only one-seventh of the total adsorbed Ca^{2+} ions.

Since the adsorption of Ca^{2+} and SO_4^{2-} ions onto Mand C–S–H surfaces is similar, while LP surfaces have higher affinity for Ca^{2+} ions tn SO_4^{2-} ions, it is concluded that calcite surfaces have much higher affinity for Ca^{2+} ions than MS and C–S–H surfaces. This can be explained by the different adsorption mechanisms of Ca^{2+} ions onto MS and LP surfaces. In the case of LP, it is believed that the adsorption driving force is entirely enthalpy-governed, and the adsorption of Ca^{2+} ions onto LP surfaces is due to a moderately strong acid–base (donor–acceptor) interaction between the adsorbing Ca^{2+} ion and the active surface site [28]. This chemical interaction could result in a strong adsorption of calcium ions onto calcite surfaces and low mobility of those adsorbed Ca^{2+} ions, as previously discussed in [34]. Whereas, the adsorption of Ca^{2+} ions onto the silica surface is caused by electrostatic and non-Coulombic interactions [35]. In fact, as already suggested [36], electrostatic interaction is the main driving force for adsorption of Ca^{2+} on the surface of MS particles. This relatively weak interaction would lead to a weak adsorption of Ca^{2+} and SO_4^{2-} ions onto MS and C–S–H surfaces, consequently a relatively high mobility of those adsorbed ions. This type of interaction also plays an important role for the nucleation and growth of C–S–H phases, since the liquid phase of cement paste before setting contains a high concentration of Ca^{2+} and SO_4^{2-} ions. Although the concentration of K^+ and Na^+ ions is even higher, these ions are "indifferent" ions. The silicate concentration is very low and the aluminate concentration is even lower, as shown in Table 4. The relationship between this interaction and the nucleation and growth of C–S–H phases on the fillers' surface will be discussed in more detail in the Sect. 3.4.

3.3 Morphology of hydration products on the surface of fillers

Figure 7 shows the formation of hydrates on the surface of Portland cement (OPC), micronized sand (MS) and limestone (LP) grains. As can be observed, judging from the topography of the studied surfaces, hydrates formed in a similar way on both MS and OPC surfaces in the OPC–LP–MS paste. There is no evidence for a different state or behaviour of the cement and MS surfaces with respect to C–S–H nucleation. Figure 7a, b shows the surface of MS and OPC after 1 h 30 min of hydration. Small particles can be seen on both surfaces. The particles seem to be tiny blobs, or clusters of, most likely, C–S–H and CH nuclei. The presence of randomly distributed nuclei on micronized sand and Portland cement surfaces confirms that these surfaces act as a substrate for the heterogeneous nucleation of the hydrates. After 4 h,

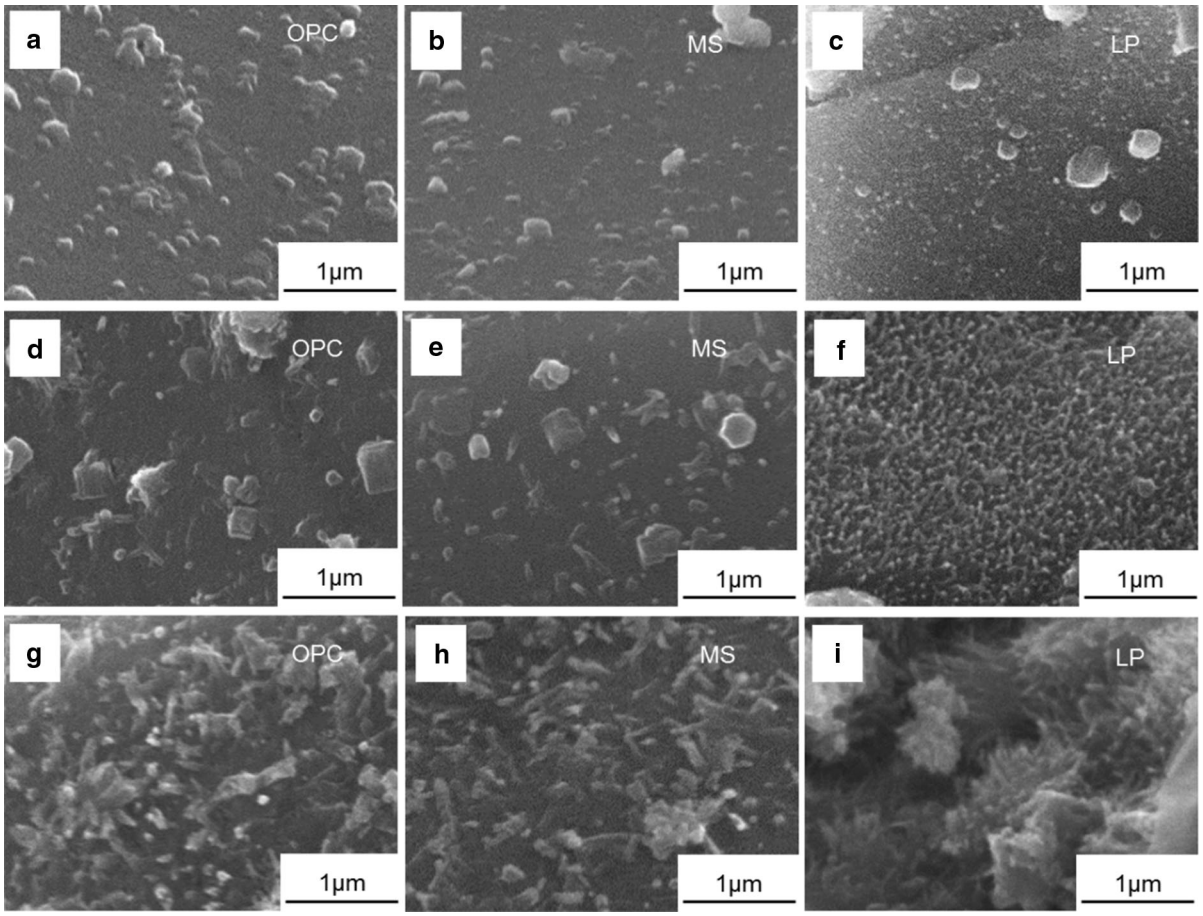

Fig. 7 Morphology of hydration products on surface of Portland cement grain at **a** 1 h 30 min **d** 4 h **g** 7 h 30 min, micronized sand grain at **b** 1 h 30 min **e** 4 h **h** 7 h 30 min and limestone grain at **c** 1 h 30 min **f** 4 h **i** 7 h 30 min

some of the C–S–H nuclei started to grow, presenting a needle shape morphology and several calcium hydroxide particles (hexagonal plates) can be identified, as shown in Fig. 7d, e. After hydration for 7 h and 30 min (Fig. 7g, h) the C–S–H crystals were well defined as needles which varied in growth orientation. As can be clearly observed, the nucleation and growth of C–S–H on micronized sand grains were very similar to that on Portland cement grains.

The micrographs in Fig. 7c, f, i clearly show that limestone had a different effect on the nucleation and growth of C–S–H, if compared to micronized sand and Portland cement. After 1.5 h hydration, the limestone surface was covered with a dense and uniform layer of C–S–H nuclei (Fig. 7c). In contrast, at equal hydration period of 1.5 h, the surfaces of micronized sand and Portland cement presented only a few dispersed nuclei (Fig. 7a, b). This microstructural observation indicates that C–S–H nucleates preferentially on the limestone surface. Figure 7f shows a limestone grain after 4 h of hydration. C–S–H needles were grown densely perpendicular to the surface, while the C–S–H crystals on the Portland cement and micronized sand grain were irregular (Fig. 7d, e). After hydration for 7 h 30 min (Fig. 7i) the C–S–H needles were already larger. The size and length of the C–S–H particles on the surface of Portland cement, micronized sand and limestone grains seemed similar with prolonged hydration. However, the layer of hydration products on the LP surface (Fig. 7i) appeared to be denser and more uniformly distributed of the crystallites, compared to these in the case of MS and OPC (Fig. 7g, h). Similar observations were reported by Berodier and Scrivener [14].

3.4 Discussion

The difference of surface charge properties between silica and calcite, i.e. zeta potential values as depicted in Figs. 3, 4, 5 and 6, is consistent with the difference in nucleation and growth of C–S–H phases on the silica and calcite surfaces (Fig. 7). This indicates the strong relationship between the surface charge properties of fillers and the mechanisms of actual C–S–H nucleation and growth.

Two types of nucleation are generally known: homogeneous and heterogeneous nucleation. Homogeneous nucleation occurs when there are no foreign constituents in a phase. Homogeneous nucleation is initiated by the saturation of the solution. In the case when foreign constituents are present in a phase, they promote the nucleation process and thereby increase the nucleation rate. In this situation the nucleation is called heterogeneous [36]. The nucleation of C–S–H on the surface of fillers is heterogeneous.

The Adsorption of nucleus constituents to the surface of the substrate affects heterogeneous nucleation [21]. The overall kinetics of crystal precipitation has to consider that the process consists of a series of consecutive steps [21]:

1. Adsorption: adsorption of constituent ions onto the substrate;
2. Surface nucleation: diffusion of adsorbed ions; partial dehydration; formation of a two-dimensional nucleus; growth to three-dimensional nucleus;
3. Crystal growth: each one of these sequential processes consists of more than one reaction step.

In this study, when OPC, LP, MS particles and water are mixed, the cement grains start to dissolve. The solution soon contains a variety of anions and cations, and ionic strength increases. The surfaces of OPC, LP and MS particles are soon charged, and the cations and anions compete with each other to absorb on these charged surfaces. As mentioned before, the concentration of Na^+, K^+, SO_4^{2-}, Ca^{2+} soon reaches concentrations of approximately 0.08, 0.2, 0.08 and 0.015 mol/L (Table 4), respectively. Although the concentration of K^+ and Na^+ ions is even higher, these ions are "indifferent" ions. The silicate concentration is very low and the aluminate concentration is even lower, The high density divalent ions, such as Ca^{2+} ions and SO_4^{2-} ions, dominate in this competition. The Ca^{2+} ions, well known to be the most important factor determining the kinetic, morphological and structural features of C–S–H, also control the nucleation characteristics within heterogeneous C–S–H nucleation [12].

As previously discussed in Sect. 3.2, the surface of LP particles possesses a much higher affinity for calcium ions than for sulfate ions due to the fact that the driving force for the adsorption of Ca^{2+} ions onto LP surfaces is entirely enthalpy-governed. This adsorption caused by a moderately strong acid–base (donor–acceptor) interaction. Because of this chemical bonding of Ca^{2+} ions (nucleus constituents) to the surface of the LP, much more calcium ions are adsorbed onto the LP surfaces and thereby more positive zeta-potential are expected. These results from zeta-potential measurements, as shown in Figs. 3, 4, 5 and 6, confirmed it. Besides, this chemical interaction could enhance the adsorption of calcium ions onto calcite surfaces and reduce the mobility of these adsorbed Ca^{2+} ions, which result in facilitating the formation of a 'stable nuclei'. This 'stable nuclei', subsequently, grows to form macroscopic particles. As a result, a large amount of C–S–H nuclei are generated on the LP surfaces, which are supported by microscopic observations of morphology and distribution of hydration products on the LP surfaces, as shown in Fig. 7. Furthermore, the C–S–H growth orientation is uniform and perpendicular to the LP surfaces (Fig. 7). This is likely to be at least partly due to the strong chemical interaction, which is able to stabilize the C–S–H crystal phase.

Different from LP, MS and OPC with similar surface properties, have no affinity for Ca^{2+} ions. The adsorption of Ca^{2+} and SO_4^{2-} ions onto MS and C–S–H surfaces is similar, which was confirmed by zeta-potential measurements, as shown in Fig. 6. The adsorption is mainly driven by electrostatic interaction. This relatively weak interaction could lead to a weak adsorption of Ca^{2+} and SO_4^{2-} ions onto MS and C–S–H surfaces and higher mobility of these adsorbed Ca^{2+}, which make these adsorbed ions diffuse into the solution again easily. As a result, less calcium ions are adsorbed onto the MS surfaces, which cause less positive zeta-potential. These were confirmed by the zeta-potential measurements, as shown in Figs. 3, 4, 5

and 6. This relatively weak interaction is unfavourable for the formation of a 'stable nuclei'. Consequently, only a few dispersed nuclei are generated on their surfaces, which are confirmed by microscopic observations of morphology and distribution of hydration products on the MS surfaces, as shown in Fig. 7. Moreover, the variation of the C–S–H growth orientation (Fig. 7) on MS surfaces is probably due to the weak electrostatic interaction, which would make the C–S–H crystal phase attached to MS surface insecure.

4 Conclusions

This paper investigated the mechanisms controlling nucleation and growth of C–S–H on the surface of OPC particles and two different filler particles (micronized sand and limestone powder). Microscopical observations of the nucleation and growth of C–S–H on these surfaces were carried out by SEM. Additionally, the surface charge properties of the two different fillers were studied using zeta potential measurements. The relation between surface (electro)chemical properties of filler and cement particles, and the nucleation and growth of C–S–H was discussed. Based on the obtained results, the following conclusions can be drawn:

1. The zeta potential test results showed that micronized sand, C–S–H and Portland cement particles have similar surface (electro)chemical properties due to the fact that they are rich in silicate. Whereas, limestone exhibits different surface charge properties. Compared to micronized sand, C–S–H and Portland cement particles, the surface of limestone particle has a higher affinity for calcium ions.
2. Microscopic observations showed that limestone has a different effect on the nucleation and growth of C–S–H compared to Portland cement and micronized sand. On the surface of limestone, a much higher density of uniformly distributed C–S–H nuclei was generated after a very short hydration time. Afterwards, C–S–H needles were growing densely perpendicular to the surface of limestone, whereas only a few dispersed nuclei were observed on both Portland cement and micronized sand surface. Furthermore, the C–S–H crystals on these surfaces were growing in different directions.
3. Our results showed a clear relation between surface chemical properties and the nucleation and growth of C–S–H. The C–S–H nucleation and growth appeared to be indeed due to the interactions between a filler surface and calcium ions in the pore solution. These interactions were determined by the chemical nature of the filler surface. The adsorption of calcium ions onto limestone particles was predominantly determined by donor–acceptor mechanisms, following moderate acid–base interactions. These strong interactions decreased the classical energy barrier, facilitating the formation of 'stable nuclei' that grows to form macroscopic particles. Consequently, a large amount of C–S–H nuclei were generated on the LP surfaces. In contrast, the adsorption of calcium ions onto micronized sand and Portland cement surfaces is mainly driven by a relatively weak electrostatic interaction, leading to less adsorbed calcium ions. This is unfavourable for the formation of 'stable nuclei', and thereby resulted in only a few dispersed nuclei on their surfaces.

This study gives an insight into the mechanisms controlling nucleation and growth of C–S–H on the surface of filler and cement particles. The research correlates and unifies the fundamental parameters that drive the filler effect and provides an understanding of the influence of fillers on nucleation and growth of C–S–H.

Acknowledgements The first author would like to gratefully acknowledge the financial support of the China Scholarship Council (CSC). The help of Dr. Chassagne Claire and Dr. Hitham Amin Hassan in zeta potential measurement is highly appreciated.

Funding This study was funded by China Scholarship Council (CSC).

Compliance with ethical standards

Conflict of interest The authors declare that they have no conflict of interest.

References

1. Bonavetti V, Donza H, Menendez G, Cabrera O, Irassar EF (2003) Limestone filler cement in low w/c concrete: a rational use of energy. Cem Concr Res 33:865–871
2. Nehdi M, Mindess S, Aitcin PC (1996) Optimization of high strength limestone filler cement mortars. Cem Concr Res 26:883–893
3. Justnes H, Dahl PA, Ronin V, Jonasson JE, Elfgren L (2007) Microstructure and performance of energetically modified cement (EMC) with high filler content. Cem Concr Compos 29:533–541
4. Lothenbach B, Le Saout G, Gallucci E, Scrivener K (2008) Influence of limestone on the hydration of Portland cements. Cem Concr Res 38:848–860
5. Bentz DP (2006) Modeling the influence of limestone filler on cement hydration using CEMHYD3D. Cem Concr Compos 28:124–129
6. Gutteridge WA, Dalziel JA (1990) Filler cement: the effect of the secondary component on the hydration of Portland cement. Cem Concr Res 20:778–782
7. Soroka I, Stern N (1976) Calcareous fillers and the compressive strength of Portland cement. Cem Concr Res 6:367–376
8. Kadri EH, Aggoun S, De Schutter G, Ezziane K (2010) Combined effect of chemical nature and fineness of mineral powders on Portland cement hydration. Mater Struct 43:665–673
9. Lawrence P, Cyr M, Ringot E (2003) Mineral admixtures in mortars: effect of inert materials on short-term hydration. Cem Concr Res 33:1939–1947
10. Oey T, Kumar A, Bullard JW, Neithalath N, Sant G (2013) The filler effect: the influence of filler content and surface area on cementitious reaction rates. J Am Ceram Soc 96:1978–1990
11. Cyr M, Lawrence P, Ringot E (2005) Mineral admixtures in mortars: quantification of the physical effects of inert materials on short-term hydration. Cem Concr Res 35:719–730
12. Garrault-Gauffinet S, Nonat A (1999) Experimental investigation of calcium silicate hydrate (C–S–H) nucleation. J Cryst Growth 200:565–574
13. Stark J, Möser B, Bellmann F (2007) Nucleation and growth of CSH phases on mineral admixtures. Advances in construction materials 2007. Springer, Berlin, pp 531–538
14. Berodier E, Scrivener K (2014) Understanding the filler effect on the nucleation and growth of C–S–H. J Am Ceram Soc 97:3764–3773
15. Poppe A-M, De Schutter G (2005) Cement hydration in the presence of high filler contents. Cem Concr Res 35:2290–2299
16. Taylor HF (1997) Cement chemistry. Thomas Telford, London
17. A. Standard, C305 (2006) Standard practice for mechanical mixing of hydraulic cement pastes and mortars of plastic consistency. In: Annual book of ASTM standards
18. Stern O (1924) The theory of the electrolytic double-layer. Z Elektrochem 30:1014–1020
19. Moulin P, Roques H (2003) Zeta potential measurement of calcium carbonate. J Colloid Interface Sci 261:115–126
20. Douglas H, Walker R (1950) The electrokinetic behaviour of Iceland Spar against aqueous electrolyte solutions. Trans Faraday Soc 46:559–568
21. Stumm W (1992) Chemistry of the solid–water interface. Wiley, New York
22. Westall J (1987) Adsorption mechanisms in aquatic surface chemistry. In: Aquatic surface chemistry: chemical processes at the particle–water interface, Wiley, New York, p 3–32, 10 fig, 6 tab, 28 ref DOE contract
23. Rothstein D, Thomas JJ, Christensen BJ, Jennings HA (2002) Solubility behavior of Ca-, S-, Al-, and Si-bearing solid phases in Portland cement pore solutions as a function of hydration time. Cem Concr Res 32:1663–1671
24. Leroy P, Devau N, Revil A, Bizi M (2013) Influence of surface conductivity on the apparent zeta potential of amorphous silica nanoparticles. J Colloid Interface Sci 410:81–93
25. Iller R (1979) The chemistry of silica. Wiley, New York
26. Anderson N, Rubin AJ (1981) Adsorption of inorganics at solid–liquid interfaces. Ann Arbor Science Publishers Inc, Collingwood
27. Somasundaran P, Agar GE (1967) The zero point of charge of calcite. J Colloid Interface Sci 24:433–440
28. Huang YC, Fowkes FM, Lloyd TB, Sanders ND (1991) Adsorption of calcium-ions from calcium-chloride solutions onto calcium-carbonate particles. Langmuir 7:1742–1748
29. Eriksson R, Merta J, Rosenholm JB (2007) The calcite/water interface: I. Surface charge in indifferent electrolyte media and the influence of low-molecular-weight polyelectrolyte. J Colloid Interface Sci 313:184–193
30. Thompson DW, Pownall PG (1989) Surface electrical-properties of calcite. J Colloid Interface Sci 131:74–82
31. Foxall T, Peterson GC, Rendall HM, Smith AL (1979) Charge determination at calcium salt/aqueous solution interface. J Chem Soc Faraday Trans 1 Phys Chem Condens Ph 75:1034–1039
32. Nachbaur L, Nkinamubanzi PC, Nonat A, Mutin JC (1998) Electrokinetic properties which control the coagulation of silicate cement suspensions during early age hydration. J Colloid Interface Sci 202:261–268
33. Viallis-Terrisse H, Nonat A, Petit J-C (2001) Zeta-potential study of calcium silicate hydrates interacting with alkaline cations. J Colloid Interface Sci 244:58–65
34. Pourchet S, Pochard I, Brunel F, Perrey D (2013) Chemistry of the calcite/water interface: influence of sulfate ions and consequences in terms of cohesion forces. Cem Concr Res 52:22–30
35. Papirer E (2000) Adsorption on silica surfaces. CRC Press, Boca Raton
36. Kalb JA (2009) Crystallization kinetics. Phase change materials. Springer, Berlin, pp 125–148